Neurobiology of Aging 135 (2024) 26–38

Contents lists available at ScienceDirect

Neurobiology of Aging

journal homepage: www.elsevier.com/locate/neuaging.org

# Longitudinal trajectories of cognitive reserve in hypometabolic subtypes of Alzheimer's disease

Fedor Levin [a,*], Michel J. Grothe [b], Martin Dyrba [a], Nicolai Franzmeier [c,d,e], Stefan J. Teipel [a,f], for the Alzheimer's Disease Neuroimaging Initiative[1]

[a] Deutsches Zentrum für Neurodegenerative Erkrankungen (DZNE), Rostock, Germany
[b] Unidad de Trastornos del Movimiento, Servicio de Neurología y Neurofisiología Clínica, Instituto de Biomedicina de Sevilla, Hospital Universitario Virgen del Rocío/CSIC/Universidad de Sevilla, Seville, Spain
[c] Institute for Stroke and Dementia Research, Klinikum der Universität München, Ludwig-Maximilians-Universität LMU, Munich, Germany
[d] Department of Psychiatry and Neurochemistry, Institute of Neuroscience and Physiology, The Sahlgrenska Academy, University of Gothenburg, Sweden
[e] Munich Cluster for Systems Neurology (SyNergy), Munich, Germany
[f] Department of Psychosomatic Medicine, Rostock University Medical Center, Rostock, Germany

ARTICLE INFO

*Keywords:*
Alzheimer's disease
Cognitive reserve
Subtypes
Mild cognitive impairment
Prodromal AD
FDG-PET

ABSTRACT

Previous studies have demonstrated resilience to AD-related neuropathology in a form of cognitive reserve (CR). In this study we investigated a relationship between CR and hypometabolic subtypes of AD, specifically the typical and the limbic-predominant subtypes. We analyzed data from 59 Aβ-positive cognitively normal (CN), 221 prodromal Alzheimer's disease (AD) and 174 AD dementia participants from the Alzheimer's Disease Neuroimaging Initiative (ADNI) from ADNI and ADNIGO/2 phases. For replication, we analyzed data from 5 Aβ-positive CN, 89 prodromal AD and 43 AD dementia participants from ADNI3. CR was estimated as standardized residuals in a model predicting cognition from temporoparietal grey matter volumes and covariates. Higher CR estimates predicted slower cognitive decline. Typical and limbic-predominant hypometabolic subtypes demonstrated similar baseline CR, but the results suggested a faster decline of CR in the typical subtype. These findings support the relationship between subtypes and CR, specifically longitudinal trajectories of CR. Results also underline the importance of longitudinal analyses in research on CR.

## 1. Introduction

Individuals with Alzheimer's disease (AD) pathology demonstrate heterogeneity in the clinical presentation, progression of the disease, as well as differences in spatial patterns of distribution of pathology markers such as atrophy and hypometabolism (Lam et al., 2013). Heterogeneity in distribution of tau, which itself may be a driver of both atrophy and hypometabolism, has also been demonstrated (Franzmeier et al., 2020; Vogel et al., 2021). Previous studies have used spatial patterns of AD-related pathology and brain atrophy to identify distinct groups of individuals with AD dementia and mild cognitive impairment (MCI) that showed differences in clinical characteristics, typically referred to as AD subtypes (Ferreira et al., 2020; Habes et al., 2020). A study from our group described hypometabolic subtypes in AD and prodromal AD patients based on spatial patterns of $^{18}$F-fluorodeoxyglucose PET (FDG-PET) signal (Levin et al., 2021). Specifically, we identified typical, limbic-predominant and cortical predominant subtypes. The typical subtype showed an AD-typical pattern of pronounced hypometabolism in temporal and parietal areas, with comparably less pronounced involvement of the medial temporal lobe. The limbic-predominant subtype demonstrated pronounced hypometabolism in the medial temporal lobe and posterior cingulate cortex, with additional involvement of temporoparietal and frontal lobe areas. The cortical-predominant subtype showed a pattern of hypometabolism similar to the typical AD subtype, but with more pronounced hypometabolism in the frontal lobe. We observed differences between

* Correspondence to: Deutsches Zentrum für Neurodegenerative Erkrankungen (DZNE) Rostock, Gehlsheimer Str. 20, 18147 Rostock, Germany.
*E-mail address:* fedor.levin@dzne.de (F. Levin).

[1] Data used in preparation of this article were obtained from the Alzheimer's Disease Neuroimaging Initiative (ADNI) database (adni.loni.usc.edu). As such, the investigators within the ADNI contributed to the design and implementation of ADNI and/or provided data but did not participate in analysis or writing of this report. A complete listing of ADNI investigators can be found at: https://adni.loni.usc.edu/wp-content/uploads/how_to_apply/ADNI_Acknowledgement_List.pdf

https://doi.org/10.1016/j.neurobiolaging.2023.12.003
Received 30 May 2023; Received in revised form 16 November 2023; Accepted 13 December 2023
Available online 19 December 2023

subtypes in cognitive performance and longitudinal cognitive decline.

Cognitive reserve (CR) is a protective factor that has been considered a potential source of the cognitive variability observed in AD (Bettcher et al., 2019). It has also been suggested that CR could explain why some AD subtypes identified in patients at similar levels of clinical severity show differences with respect to pathology measures (Ferreira et al., 2020; Poulakis et al., 2022). CR refers to mechanisms that allow some individuals to maintain cognitive performance despite pathological processes associated with aging, AD, or other disorders (Stern, 2002; Stern et al., 2020). For example, higher CR is predictive of slower than otherwise expected cognitive decline, or slower progression of MCI to AD dementia (Nelson et al., 2021). Approaches to quantifying CR include proxy measures and residual approaches (Stern et al., 2020). Proxy variables such as education or IQ characterize an individual's experience that would contribute to CR, whereas the residual approach aims to quantify the mismatch between an individual's neuropathology and cognition where cognitive performance that is better than what would be expected by the individual's pathologic burden would indicate higher CR (Nelson et al., 2021; Reed et al., 2010). Functional imaging has also been used to evaluate specific characteristics of the brain that are relevant to CR such as left frontal cortex connectivity (Franzmeier et al., 2017; Franzmeier et al., 2018) or segregation of functional networks (Ewers et al., 2021).

In addition to cross-sectional measurements of CR, longitudinal assessments have been used to evaluate differences between participants in susceptibility to clinical progression and cognitive decline. Longitudinal change in residual memory variance – a measure of CR – was a better predictor of incident dementia than a cross-sectional measure as shown in a study by Zahodne and colleagues (Zahodne et al., 2015). Similarly, change in CR over time as assessed via latent variable models predicted clinical progression and cognitive performance in a sample ranging from cognitively normal participants to participants with mild dementia (Bettcher et al., 2019).

In the present research, we investigated the relationship between the subtype heterogeneity and CR. We addressed the question about whether the major subtypes of AD-related neurodegeneration – the typical and the limbic-predominant subtypes – showed differences in CR; and whether these differences could explain trajectories of cognitive decline or predict conversion from prodromal AD to AD dementia. We also addressed the question about whether potential differences in CR could explain characteristics of the subtypes themselves as suggested in the past research that considered the role of CR in atrophy-based subtypes in AD dementia (Persson et al., 2017; Poulakis et al., 2022). We considered a similar possibility – if one hypometabolic subtype showed less pronounced cerebral damage than another subtype at a similar level of cognitive impairment, it could be related to lower CR of participants within that subtype. In this study we were primarily interested in assessing CR in amyloid beta-positive cognitively normal (Aβ-positive CN) participants who would represent preclinical Alzheimer's pathological change and in Aβ-positive participants with MCI who would represent prodromal AD. However, we also characterized subtype characteristics and potential subtype differences in CR in the AD dementia group to provide additional context.

To quantify CR, we adapted a residual-based approach (Jack et al., 1997; van Loenhoud et al., 2019; van Loenhoud et al., 2017). Residuals in such an approach can be obtained from a regression model predicting cognitive performance from pathological brain changes (Zahodne et al., 2015) or from a model predicting levels of neuropathology from cognitive performance (van Loenhoud et al., 2019). To characterize the degree of neuropathological change, we selected grey matter (GM) volume in temporoparietal area corresponding to the typical AD atrophy (Ossenkoppele et al., 2015). Additionally, we aimed to evaluate CR residuals based on hippocampal and global GM volumes. Despite the focus of the study on CR in Aβ-positive CN and prodromal AD, the data from AD dementia participants were included in regression models used for estimating residual CR to represent a wider continuum of AD-related neurodegeneration.

To address the research questions of the current study, we tested whether hypometabolic subtypes differed in CR as expected based on the previous studies, and whether CR residuals together with subtype classification predicted progression from prodromal AD to AD dementia or cognitive decline in participants enrolled in the Alzheimer's Disease Neuroimaging Initiative (ADNI). Following that, longitudinal CR residuals would be analyzed to investigate potential differences in CR trajectories between the typical and limbic-predominant hypometabolic subtypes. Finally, we aimed to assess the replicability of findings on CR and hypometabolic subtypes in a separate ADNI3 sample. Current approach leverages different imaging modalities available in ADNI by defining subtypes using FDG-PET which is likely more sensitive to early neurodegenerative changes than measures of atrophy assessed with MRI (Kljajevic et al., 2014), and by using the residual CR measure based on GM volumes obtained from MRI scans, including longitudinal assessments.

## 2. Methods

### 2.1. Participants

The main analysis sample included 59 amyloid-positive CN, 221 prodromal AD (amyloid positive MCI participants) and 174 amyloid-positive AD participants from ADNI and ADNIGO/2 (henceforth referred to as the "main ADNI sample").

To assess replicability of findings, we also analyzed data from a separate sample of participants selected from the ADNI3 phase of ADNI. CN, prodromal AD and AD dementia participants were selected if they had FDG-PET scans, matching MRI scans and cognitive data, as well as a finding of amyloid positivity (henceforth referred to as the "ADNI3 sample"). The resulting sample included 5 amyloid-positive CN, 89 prodromal AD and 43 AD dementia participants.

Amyloid positivity in both samples was established based on $^{18}$F-florbetapir PET (AV45-PET) or $^{18}$F-florbetaben (FBB-PET) standardized uptake value ratios (SUVR) with whole cerebellum as a reference region available via the ADNI PET core (Jagust Lab, UC Berkeley). We used recommended thresholds of 1.11 for AV45 (Landau et al., 2014) or 1.08 for FBB (Royse et al., 2021) to select Aβ-positive participants. We also used available CSF amyloid data (Aβ [1–42]) as obtained using Elecsys cobas e 601,[2] to select amyloid-positive participants in cases when amyloid-sensitive PET data was not available (Grothe et al., 2021). Specifically, we selected participants with the values under the cutoff of 880 pg/ml (Hansson et al., 2018). Additionally, we used APOE ε4 information (Saykin et al., 2010) to code a binary variable showing presence of at least one APOE ε4 allele in order to account for it in statistical analyses.

The inclusion criteria for diagnostic groups in ADNI have been described previously (Teipel and Grothe, 2015). Specific inclusion criteria for different groups within the ADNI study are listed on the ADNI website (https://adni.loni.usc.edu/methods/documents/). The ADNI was launched in 2003 as a public-private partnership, led by Principal Investigator Michael W. Weiner, MD. The ADNI is a longitudinal multicenter study aimed at investigating whether neuroimaging methods such as MRI and PET, together with other biological, genetic,

[2] The Elecsys β-Amyloid(1−42) CSF immunoassay in use is not a commercially available IVD assay. It is an assay that is currently under development and for investigational use only. The measuring range of assay is 200 (lower technical limit) – 1700 pg/ml (upper technical limit). The performance of the assay beyond the upper technical limit has not been formally established. Therefore, use of values above the upper technical limit, which are provided based on an extrapolation of the calibration curve, is restricted to exploratory research purposes and is excluded for clinical decision making or for the derivation of medical decision points.

clinical and neuropsychological measures can be used to characterize progression of mild cognitive impairment (MCI) and early Alzheimer's disease (AD). For up-to-date information, see https://adni.loni.usc.edu.

### 2.2. Neuropsychological test scores

ADNI data includes neuropsychological tests covering different domains. For analysis of cognitive performance, we used established cognitive composite scores for memory (ADNI-MEM) (Crane et al., 2012) and executive function (ADNI-EF) (Gibbons et al., 2012). The ADNI-MEM composite score was used for calculating residuals to represent an estimate of CR. Mini Mental State Examination (MMSE) scores were used for characterizing global cognitive impairment. Clinical dementia rating (CDR) scores were used to assess progression from prodromal AD to AD dementia (defined as a change in the score from 0.5 to $\geq$ 1.0). To characterize longitudinal cognitive performance in the Aβ-positive CN and prodromal AD participants in the main ADNI sample, we analyzed ADNI-MEM and ADNI-EF data with available follow-up of up to 114 months and with a mean follow-up period of 53 $\pm$ 29 months. In the replication ADNI3 sample, we analyzed longitudinal data from the Aβ-positive CN and prodromal AD with a maximal follow-up of 49 months and a mean follow-up of 24 $\pm$ 10 months.

### 2.3. FDG-PET data analysis and assignment into subtypes

Pre-processed FDG-PET images were obtained from the ADNI server. For a more detailed description of acquisition and standardized image pre-processing steps please refer to the ADNI website (https://adni.loni.usc.edu/methods/documents/). The images were additionally normalized to a customized FDG-PET template and smoothed with a Gaussian kernel of 8 mm full-width at half maximum (Lange et al., 2016; Levin et al., 2021). As in our previous study, subtypes were defined using Ward's hierarchical clustering of individual voxel-wise FDG-PET profiles (Levin et al., 2021). Clustering analyses were implemented in MATLAB. Individual voxel-wise FDG-PET profiles of participants were normalized to the global mean signal to account for possible differences in the overall hypometabolism severity prior to clustering or classification. Following our previous study (Levin et al., 2021), a cutoff at the level of three clusters was applied yielding a typical, a limbic-predominant and a cortical-predominant subtype. Amyloid-positive CN participants and prodromal AD participants from the main ADNI sample, as well as participants from the replication ADNI3 sample, were classified based on their similarity to AD dementia clusters. Briefly, each participant's individual FDG-PET profile was categorized into a corresponding AD subtype based on Euclidean distance to the mean profiles of the typical, limbic-predominant and cortical-predominant subtypes. Due to low participant numbers in the cortical-predominant subtype (n = 12 in the AD group and n = 2 in the prodromal AD group in the main ADNI sample), it was omitted from statistical analyses, which instead focused on differences between the typical and the limbic-predominant subtypes.

For visualizing hypometabolic patterns of the typical and the limbic-predominant subtypes, we conducted two-sample voxel-wise t-tests comparing the respective subtypes to an Aß-negative CN group (n = 120), applying scaling to the pons reference signal, and including age, sex and years of education as covariates to visualize the patterns independently of possible differences in these demographic characteristics. Additionally, we directly compared the typical and the limbic-predominant subtypes by using two-sample voxel-wise t-tests, applying scaling to the pons reference signal, and including age, sex, years of education and MMSE as covariates. Please note, that scaling to pons signal for the purpose of visualizing subtypes here differs from scaling to the average signal used for the clustering procedure. Statistical parametric maps of the group differences were converted into Z-score maps using CAT12.8 (Gaser et al., 2023).

### 2.4. MRI scan preprocessing and volumetric analysis

Structural MRI scans (including scans obtained with 1.5 T scanners in ADNI1 and scans obtained with 3 T scanners in other ADNI phases) were used to obtain measures of GM volumes in selected brain areas. For details about collection of the MRI data in ADNI, please refer to the documentation at the website (https://adni.loni.usc.edu/methods/documents/). We used separate preprocessing pipelines for the baseline and for the longitudinal MRI data. The baseline MRI data were preprocessed with the CAT12.8 (Gaser et al., 2023) segmentation pipeline implemented within SPM12 toolbox (Wellcome Trust Center for Neuroimaging) and spatially normalized using DARTEL (Diffeomorphic Anatomical Registration Through Exponentiated Lie algebra).

We selected follow-up MRI scans that were available for a subset of the main ADNI sample, including 44 Aβ-positive CN, 175 prodromal AD and 105 AD dementia participants. Follow-up MRI data from AD dementia participants were included to obtain GM volume estimates using the same longitudinal pipeline as for other participants to later include in the regression model used for obtaining longitudinal W-scores. Scans were obtained for delays of approximately 1, 2 or 4 years after the baseline, with an average of 1.8 follow-up scans per participant in addition to the baseline scan. MRI scans collected at delays of about 3 years were omitted from this analysis due to the drop in the number of available scans (37 available a 3-year delays, compared to 157 at 2 years and 77 at 4 years; excluding the cortical-predominant subtype). Longitudinal data available within the ADNI3 sample included 3 Aβ-positive CN and 53 prodromal AD participants with available MRI follow-ups, and we selected MRI scans obtained at delays of approximately 1, 2, 3 and 4 years after the baseline, with an average of 1.6 follow-up scans. For one participant in the main ADNI sample and for 6 participants in the ADNI3 sample there were no cognitive composites found that corresponded to follow-up MRI scans. The baseline data from these participants were still included in the longitudinal models of progression of CR residuals.

Longitudinal MRI data were preprocessed using the CAT12.8 longitudinal segmentation pipeline with a setting optimized for detecting large changes such as atrophy (Gaser et al., 2023). The longitudinal pipeline also used the DARTEL algorithm as a setting for spatial registration. Scans were evaluated for segmentation errors and two participants from the ADNI3 sample were excluded from the longitudinal MRI analyses and one other participant was excluded from the baseline data analyses. We obtained temporoparietal (for the exact list of the included atlas labels, see Supplementary table 1) and hippocampal bilateral masks that were defined in the AAL3 atlas (Rolls et al., 2020; Tzourio-Mazoyer et al., 2002) available with the CAT12.8 toolbox, as well as global GM volumes, and thresholded them at 0.5 template GM probability. We extracted GM volume from the regions of interest using modulated normalized GM maps and divided the values by the individual total intracranial volume (TIV) at baseline (Dyrba et al., 2021).

In some cases, MRI data within one participant were collected using different scanner models. We included a variable indicating participants with a change in the scanner as a covariate in the longitudinal regression analyses of CR residuals.

### 2.5. Calculation of CR residuals

We calculated standardized residuals as a measure of CR (van Loenhoud et al., 2019). We used a regression model in which individual cognitive performance at baseline represented by the ADNI-MEM score was predicted by the temporoparietal GM volume adjusted to the TIV, and covariates – age and sex. Temporoparietal GM volume has been previously used for obtaining W-scores based on standardized residuals in a model predicting atrophy (van Loenhoud et al., 2019), and we also selected this measure because temporoparietal regions show common atrophy across distinct AD phenotypes (Ossenkoppele et al., 2015). Despite differences in spatial patterns of hypometabolism of subtypes,

we used common atrophy measures across participants to be able to directly compare the differences in CR between the subtypes. Regression model in the current study used the main ADNI sample data including Aβ-positive CN, prodromal AD and AD dementia participants to take into account the relationship between neurodegeneration and cognitive performance throughout the clinical continuum of the disease. Including AD participants ensures that there are sufficient data in the model to characterize the relationship between neurodegeneration and cognitive performance at lower values of either measure. The data contributing to the model and the plotted predicted values from the regression model are presented in Figure 1. For a given participant, a positive residual as obtained directly in the regression model would correspond to cognitive performance higher than expected given the neurodegeneration measure and covariates, therefore indicating higher CR than for a participant with a lower value of the residual. We multiplied residual values by − 1 so that higher values of the residual estimates of CR would correspond to better than expected cognitive performance. We standardized individual residuals dividing them by the residual standard error of the sample used for the model.

In the ADNI3 sample, we obtained CR residuals by applying the same calculation as used in the main ADNI sample. We used the intercept and regression coefficients from the regression model from the main ADNI sample to calculate ADNI-MEM values that would have been predicted by this model for ADNI3 participants. Then the differences between observed and predicted values for the participants in the ADNI3 sample were standardized by being divided by the residual standard error from the model using the main ADNI sample. This calculation was done in the consistent manner with CR residuals in the main ADNI sample to ensure direct comparability of the measures. For comparisons, we also calculated analogous models: one based on using temporoparietal FDG-PET signal (adjusted to pons) in the main ADNI sample and another based on temporoparietal GM volume in the ADNI3 baseline data alone.

For the analysis of the longitudinal trajectories of CR, we calculated longitudinal CR residuals in the subsample of participants who had available longitudinal MRI data, as well as cognitive composite scores. Specifically, we first selected the baseline visit data from Aβ-positive CN, prodromal AD and AD dementia participants who had available follow-up MRI scans, because only for them longitudinal temporoparietal GM volume values could be obtained from the longitudinal MRI segmentation. These data were used in a regression model analogous to the main baseline model for CR residuals. Intercept and regression coefficients from this regression model were then used with follow-up data to calculate longitudinal CR residuals in the main ADNI sample and in the ADNI3 sample. Specifically, for each follow-up entry with available MRI and ADNI-MEM data we consistently calculated the CR residual measure in the same manner.

In complementary analyses, we considered alternative approaches to defining CR residuals, specifically using GM volumes extracted from other brain areas to represent neurodegeneration measures such as hippocampal and global GM atrophy with baseline and longitudinal data (referred to as “CR residuals – hippocampal GM” and “CR residuals – global GM” respectively) (van Loenhoud et al., 2019). Longitudinal versions of CR residuals using hippocampal and global GM volumes were also analyzed in similar longitudinal regression models.

### 2.6. Statistical analysis

We conducted statistical analyses using R (version 4.1.3) accessed via RStudio. Characteristics of subtypes within groups were compared using Mann–Whitney U test or Chi-squared tests (for sex and APOE ε4 prevalence). We tested the relationships between years of education and various versions of baseline CR residuals using partial correlations with age, sex and a variable indicating AD dementia status as covariates. AD dementia status was included as a control variable because previous publications have suggested a possible acceleration of cognitive decline in AD dementia patients with higher CR (Stern, 2012; van Loenhoud et al., 2019). This could result in a decrease in W-scores in some participants leading to a stronger discrepancy with education representing premorbid CR in the AD dementia group.

To evaluate risk of clinical progression depending on subtype and CR residuals, we used survival analysis with progression from prodromal AD to AD defined as a change from CDR score 0.5 to ≥ 1.0 (Teipel et al., 2020). The Cox proportional hazards model included W-scores, subtype variable, interaction between them, as well as sex, age, and APOE ε4 as covariates.

To assess whether CR residuals predicted longitudinal cognitive performance change, we used linear mixed effects regression models (Levin et al., 2021) in the subsample of Aβ-positive CN and prodromal AD participants. Linear mixed effects regression models were used to assess differences in longitudinal changes in memory, executive function, and global cognitive performance assessed via MMSE scores. Models included time of follow-up measured in years from baseline, CR residuals, a binary variable indicating the limbic-predominant subtype and an interaction term for these variables. Interaction between CR residuals and time indicated an effect of CR residuals on cognitive trajectories over time, whereas an interaction between CR residuals, time and subtype indicated potential difference between the subtypes with respect to the benefit of higher W-scores for longitudinal cognitive performance. Age, sex, APOE ε4 and interaction of age with the time variable were included as covariates. The resulting models were specified with the following variables and interactions: Y = Time*CR residuals*Subtype + Time*CR residuals+ Time*Subtype + CR

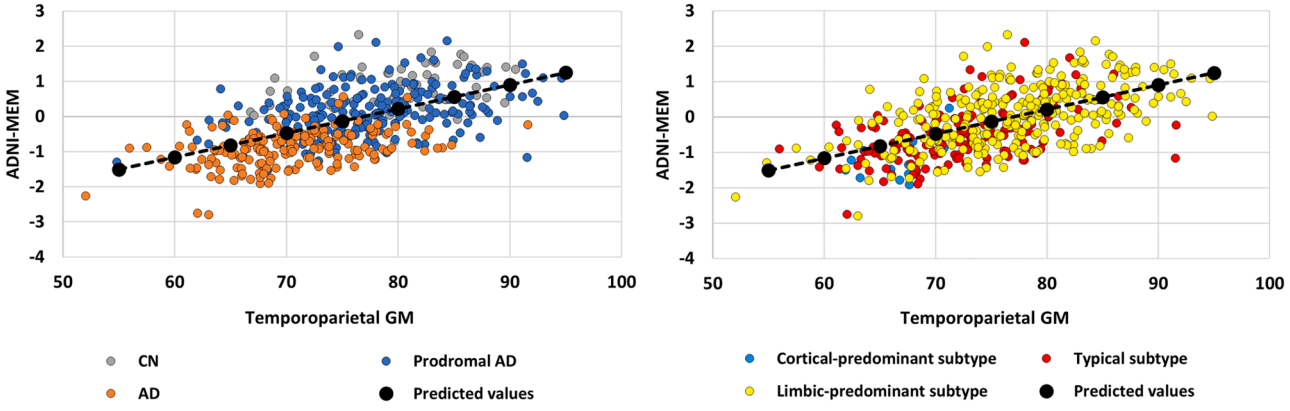


**Figure1. Regression model used for defining CR residuals.** Regression model predicting memory (ADNI-MEM) composite scores from temporoparietal GM volumes and covariates. Lines represents values predicted by the model for a woman with average age (74y). Positive residuals (above individual predicted values) correspond to higher residuals and indicate higher CR. On the left – datapoints split by group, on the right – datapoints split by hypometabolic subtypes.

residuals*Subtype + Time*Age + Time + CR residuals+ Subtype + Age + Sex + APOE ε4. Regression models included random intercepts for participants and random slopes for the time variable. The age variable was centered and rescaled by standard deviation. In the ADNI3 sample, the longitudinal models predicting memory and CR residuals obtained using the hippocampal volume prompted warnings of a singular fit indicating a potential issue with overfitting. Therefore, in the ADNI3 sample we only report mixed effects models with random intercepts, but not random slopes. Additionally, we also considered analogous models without the subtype variable and corresponding interactions to assess the potential protective effect of CR residuals across the subtypes.

We assessed differences between the subtypes with respect to the longitudinal change of W-scores using mixed effects models with longitudinal CR residuals as a dependent variable. Models included time of follow-up measured in years from baseline, a binary variable indicating the limbic-predominant subtype, and an interaction term for time by subtype as independent variables. Interaction between subtype and time indicated whether subtypes differed in trajectories of CR residuals over time, with age, sex, APOE ε4, a variable indicating a change in scanner as covariates and an interaction term for age and time. The resulting models included following variables and interactions: Y = Time*Subtype + Time*Age + Time + Subtype + Age + Sex + APOE ε4 + Scanner change. We additionally used similar models but limited to prodromal AD participants to rule out the possibility of results being driven by the Aβ-positive CN group. We also used a mixed effects regression model to compare the subtypes with respect to the longitudinal temporoparietal GM volume change to provide additional context to the analysis of CR residuals. To examine a potential confounding effect of using age as a covariate, we evaluated versions of regression models that excluded it. Additionally, we evaluated performance of FDG-PET-based CR residuals in models of longitudinal change in cognitive performance to verify consistency of the results using this measure.

## 3. Results

### 3.1. Hypometabolic subtypes

Characteristics of hypometabolic subtypes across the main ADNI and ADNI3 samples are presented in Tables 1 and 2 and Supplementary tables 2 and 3, respectively. Comparisons of FDG-PET patterns of the typical and limbic-predominant subtypes to the Aß-negative CN group are presented in the Figure 2. Direct comparisons of FDG-PET patterns between the typical and limbic-predominant subtypes in the main ADNI and in the ADNI3 samples are presented in Supplementary figures 1 and 2. Characteristics of the hypometabolic subtypes in AD dementia have also been described previously (Levin et al., 2021). In the replication ADNI3 sample, some differences between the subtypes followed a generally similar pattern to the one previously observed in the main ADNI sample. For example, the limbic-predominant subtype in the AD dementia group as compared to the typical subtype was on average older (77.5 vs 73 years, $p = 0.179$) and showed higher baseline executive function performance ($p = 0.028$; Supplementary table 2).

### 3.2. CR residuals and education

Confirming the expected relationship between our residual measure of CR and the commonly used proxy measure of CR, CR residuals positively correlated with years of education in a partial correlation including covariates age, sex and AD dementia status (main ADNI sample: $r = 0.16$; $p < 0.001$; ADNI3 sample: $r = 0.26$; $p = 0.002$). The regression model in the main ADNI sample used for defining the CR residuals had adjusted $R^2 = 0.33$; resulting CR residuals correlated with ADNI-MEM scores with $r = 0.81$ ($p < 0.001$). The regression model predicting ADNI-MEM from temporoparietal FDG-PET defined in the main ADNI sample and the model predicting ADNI-MEM from temporoparietal GM defined in the baseline ADNI3 sample demonstrated parameters similar to the main model defined in the main ADNI sample that was used for deriving the CR residuals based on temporoparietal GM volume (please see Supplementary table 4).

To evaluate the potential contribution of the selected neurodegeneration measure to the observed subtype differences in CR we considered alternative approaches for deriving CR residuals – using the hippocampal and global masks to assess GM volume alternative to the temporoparietal mask as used in the main CR residuals model. All versions of CR residuals correlated with each other and with years of education in partial correlations controlling for age, sex and AD dementia status (all $p \leq 0.001$).

**Table 1**
Demographic, clinical and biomarker characteristics of AD dementia subtypes in the main ADNI sample at baseline.

| | Typical | Limbic-predominant | Cortical-predominant | P-value, typical vs limbic-predominant |
|---|---|---|---|---|
| **Demographics** | | | | |
| n (%) | 84 (48.3%) | 78 (44.8%) | 12 (6.9%) | |
| Age, years | 74.2 (8.5) | 76 (6.7) | 67.9 (7.1) | 0.263 |
| Sex, female (%) | 39% | 49% | 50% | 0.293 |
| Education, years | 15.6 (2.6) | 15.3 (3.1) | 16.7 (2.5) | 0.797 |
| **Cognition** | | | | |
| MMSE | 23.2 (2.3) | 23.4 (1.9) | 22.1 (2.2) | 0.518 |
| ADNI-MEM | -0.91 (0.49) | -0.85 (0.56) | -1.31 (0.44) | 0.515 |
| ADNI-EF | -1.1 (0.87) | -0.66 (0.88) | -1.68 (0.74) | 0.002 |
| **Biomarkers** | | | | |
| APOE ε4 (%) | 79% | 81% | 58% | 0.912 |
| AV45-PET SUVR | 1.47 (0.17) | 1.44 (0.15) | 1.41 (0.17) | 0.374 |
| CSF Aβ, pg/ml | 584 (229) | 596 (166) | 645 (142) | 0.177 |
| Temporoparietal GM | 69.52 (5.62) | 72.4 (6.5) | 66.01 (2.7) | < 0.001 |
| Hippocampal GM | 3.71 (0.45) | 3.6 (0.61) | 4.04 (0.49) | 0.259 |
| Global GM | 299.06 (18.5) | 300.71 (23.24) | 289.19 (15.31) | 0.263 |
| **CR** | | | | |
| CR residuals – temporoparietal GM | -0.49 (0.78) | -0.73 (0.74) | -0.65 (0.59) | 0.053 |
| CR residuals – hippocampal GM | -0.64 (0.82) | -0.49 (0.84) | -1.44(0.76) | 0.199 |
| CR residuals – global GM | -0.68 (0.74) | -0.68 (0.69) | -0.85 (0.57) | 0.911 |

Sample sizes are presented with percentages relative to the group in parentheses. GM volumes are scaled to TIV. Values for variables are presented as percentages (for sex and APOE ε4 genotype) or means with standard deviation in parentheses. Missing values are excluded. Subtypes are compared using Mann–Whitney U tests, apart from sex and APOE ε4 prevalence which were compared using Chi-squared tests.

### 3.3. CR and hypometabolic subtypes

We assessed potential differences in CR between the subtypes, as well as interactions between CR and subtypes in regression analyses predicting longitudinal cognitive decline and clinical progression. Contrary to the expected effect, the typical and the limbic-predominant subtypes in the Aβ-positive CN, prodromal AD and AD dementia groups in the main ADNI and in the ADNI3 samples did not demonstrate significant differences in education (Tables 1 and 2, Supplementary tables 2 and 3).

**Table 2**
Demographic, clinical and biomarker characteristics of amyloid-positive CN and prodromal AD subtypes in the main ADNI sample at baseline.

| | Amyloid-positive CN participants | | Prodromal AD participants | | | |
|---|---|---|---|---|---|---|
| | Typical | Limbic-predominant | Typical | Limbic-predominant | Cortical-predominant | P-value, prodromal AD typical vs limbic-predominant |
| **Demographics** | | | | | | |
| n (%) | 6 (10%) | 53 (90%)) | 57 (25.8%) | 162 (73.3%) | 2 (0.9%) | |
| Age, years | 74.1 (6.1) | 76.9 (6) | 70.8 (6.5) | 74.1 (6.8) | 76.4 (0.57) | 0.006 |
| Sex, female (%) | 33% | 60% | 42% | 44% | 0% | 0.880 |
| Education, years | 17.5 (2.3) | 16 (2.6) | 16.5 (2.5) | 15.9 (3.0) | 17 (1.41) | 0.180 |
| **Cognition** | | | | | | |
| MMSE | 28.7 (1.5) | 29 (1) | 27.4 (1.8) | 27.8 (1.8) | 28 (2.8) | 0.145 |
| ADNI-MEM | 0.51 (0.67) | 0.9 (0.58) | 0.04 (0.72) | 0.21 (0.65) | -0.07 (0.46) | 0.056 |
| ADNI-EF | 0.49 (0.78) | 0.59 (0.70) | 0.29 (1.03) | 0.22 (0.87) | -1.4 (0.35) | 0.826 |
| **Biomarkers** | | | | | | |
| APOE ε4 (%) | 50% | 38% | 72% | 64% | 50% | 0.369 |
| AV45-PET SUVR | 1.29 (0.21) | 1.32 (0.18) | 1.42 (0.16) | 1.37 (0.18) | 1.5 (0.28) | 0.023 |
| CSF Aβ, pg/ml | 650 (218) | 948 (548) | 758 (375) | 788 (330) | 775 (258) | 0.299 |
| Temporoparietal GM | 78.62 (5.07) | 79.95 (6.18) | 76.69 (5.44) | 78.01 (7.12) | 71.78 (0.78) | 0.121 |
| Hippocampal GM | 4.4 (0.51) | 4.55 (0.49) | 4.27 (0.54) | 4.2 (0.61) | 4.06 (0.12) | 0.702 |
| Global GM | 312.22 (16.7) | 322.25 (22.35) | 318.38 (18.11) | 318.42 (24.79) | 296.94 (8.93) | 0.964 |
| **CR** | | | | | | |
| CR residuals – temporoparietal GM | 0.61 (0.94) | 0.97 (0.83) | 0.18 (1.02) | 0.25 (0.88) | 0.47 (0.72) | 0.590 |
| CR residuals – hippocampal GM | 0.53 (0.93) | 0.80 (0.83) | 0.12 (0.93) | 0.35 (0.83) | 0.09 (0.80) | 0.079 |
| CR residuals – global GM | 0.84 (0.96) | 1.05 (0.77) | 0.14 (0.98) | 0.31 (0.83) | 0.43 (0.39) | 0.179 |

Sample sizes are presented with percentages relative to the group in parentheses. GM volumes are scaled to TIV. Values for variables are presented as percentages (for sex and APOE ε4 genotype) or means with standard deviation in parentheses. Missing values are excluded. Subtypes in prodromal AD participants are compared using Mann–Whitney U tests, apart from sex and APOE ε4 prevalence which were compared using Chi-squared tests. Amyloid-positive CN participants were not compared due to low number of participants in the typical subtype.

The limbic-predominant subtype in the main ADNI sample AD group demonstrated somewhat lower level of CR residuals on average; but this result was not statistically significant ($p = 0.053$).

In the Cox proportional hazards model, the effect of CR residuals in the reference typical subtype suggested that higher residuals had a protective effect (HR = 0.54; $p = 0.004$; Table 3). An interaction of CR with the subtype variable indicating limbic-predominant subtype did not show a significant effect (HR = 1.22, $p = 0.458$) suggesting a lack of subtype differences with respect to the effect of CR residuals. In the analyses in the ADNI3 sample, the effects of CR residuals in the typical subtype and the interaction term of CR residuals and the subtype variable were not statistically significant, potentially due to the small sample size.

Higher CR residuals were associated with a slower ADNI-EF and MMSE decline in a mixed effects regression model in the main ADNI sample as indicated by the interaction term for time and CR residuals ($p = 0.047$ and $p < 0.001$ respectively; see Supplementary table 5). The same effect in the model predicting ADNI-MEM was in a similar direction but not significant ($p = 0.08$). Subtypes did not significantly differ with respect to an effect of CR residuals on longitudinal cognitive decline as indicated by the interaction term (see Table 4 and Figure 3, for the version with individual data plotted see Supplementary figure 3). However, the coefficient estimates and corresponding CI for the model predicting ADNI-EF and MMSE scores indicated a potential higher benefit of CR residuals for the longitudinal progression of the typical subtype (with $p = 0.082$ and $p = 0.060$, respectively). In the ADNI3 sample (Supplementary table 6), such an effect was not supported.

We observed differences in longitudinal trajectories of change in CR between the subtypes in the predementia cohort (Aβ-positive CN and prodromal AD) of the main ADNI sample – the limbic-predominant subtype did not seem to show a pronounced longitudinal decline over time, but the typical subtype did (Table 5, Supplementary table 7, Figure 4, for the version with individual data plotted see Supplementary figure 4). The statistical test for this interaction did not yield a significant result for the CR residuals based on temporoparietal GM volume ($p = 0.054$). However, supporting the faster decline of CR in typical subtype, alternative CR residuals declined significantly faster for the typical subtype compared to the limbic-predominant subtype (for hippocampal GM CR residuals: $p = 0.025$; for global GM CR residuals: $p = 0.037$; Supplementary table 7). These effects were not supported in the replication ADNI3 sample (Supplementary table 8) – likely due to the limited sample size. Specifically, the interaction term suggested weak effects for all three CR residuals variants that were also not statistically significant ($p = 0.652$, $p = 0.579$ and $p = 0.626$ for CR residuals based on temporoparietal, hippocampal and global GM volumes respectively). In a longitudinal regression model limited to prodromal AD participants from the main ADNI sample, the results showed a similar pattern to the model with both Aβ-positive CN and prodromal AD participants (Supplementary table 9). Therefore, it is unlikely that this result was driven mainly by the inclusion of Aβ-positive CN participants who were predominantly (90% of Aβ-positive CN participants) assigned to the limbic-predominant subtype. An additional comparison of the longitudinal change in temporoparietal GM suggested a slower decline for the limbic-predominant subtype ($p = 0.024$; Supplementary table 10). Exclusion of the age covariate did not seem to have noticeable effect on regression model results (Supplementary tables 11 and 12). Finally, alternative versions of regression models examining cognitive decline that used FDG-PET-based CR residuals instead of GM-based measures demonstrated largely consistent results (Supplementary table 13).

## 4. Discussion

The current study investigated the relationship between CR and hypometabolic subtype heterogeneity within groups of Aβ-positive CN, prodromal AD and AD dementia participants. The two examined major hypometabolic subtypes – the typical and the limbic-predominant subtypes – differed at baseline with respect to the temporoparietal GM volume ($p < 0.001$), but not ADNI-MEM. It is likely that this contributed to the average CR residuals for the typical subtype being somewhat higher in the AD group, although non-significantly ($p = 0.053$).

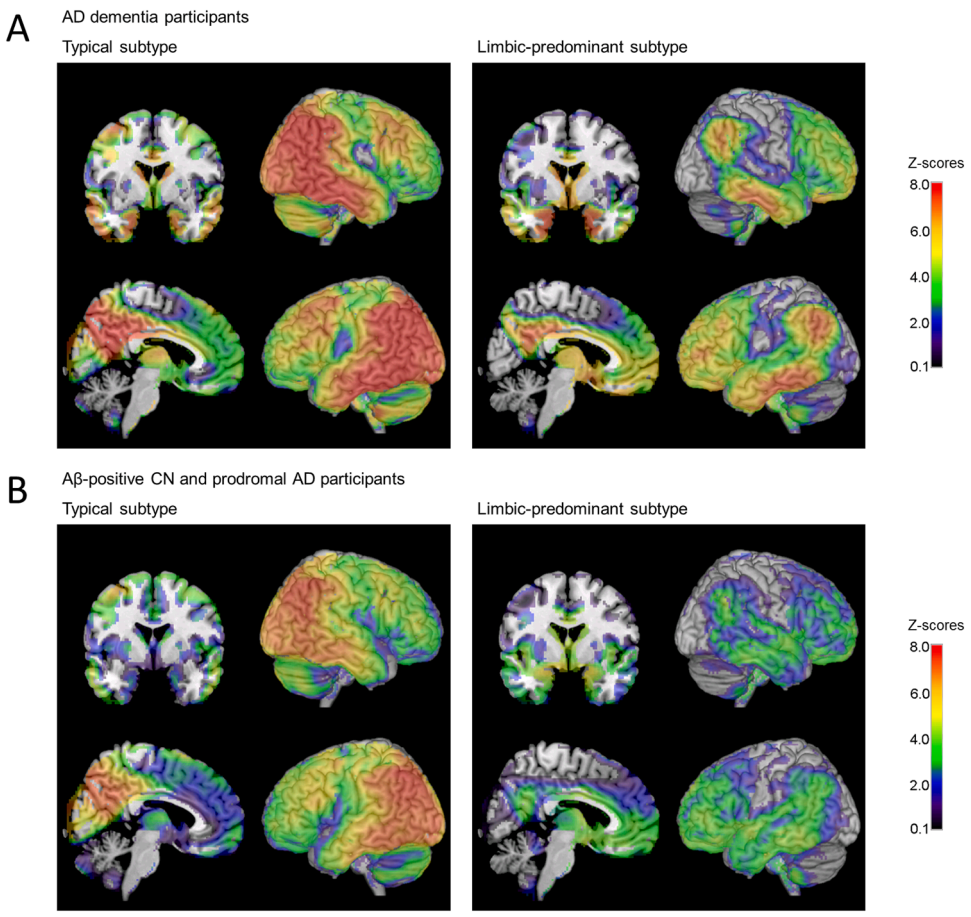


**Fig. 2. Hypometabolic FDG-PET patterns of subtypes in the main ADNI sample.** Voxel-wise hypometabolic patterns of the typical and limbic-predominant subtypes were compared to Aβ-negative CN group (n = 120) in (A) AD dementia participants and (B) Aβ-positive CN and prodromal AD participants. FDG-PET scans were scaled to the pons reference signal, age, sex and years of education were used as covariates. Statistical parametric maps of the group differences were converted into Z-scores.

**Table 3**
Hazard ratios for progression of subtypes of participants with prodromal AD to dementia in the main ADNI sample and in the ADNI3 sample.

| | Main ADNI sample | | | ADNI3 sample | | |
|---|---|---|---|---|---|---|
| Variable | HR | CI | z-statistic | HR | CI | z-statistic |
| CR residuals – temporoparietal GM | 0.54 * * | 0.35, 0.82 | -2.85 | 0.23 | 0.01, 3.92 | -1.01 |
| Limbic-predominant subtype | 0.52 * | 0.30, 0.89 | -2.40 | 0.09* | 0.01, 1.00 | -1.96 |
| CR residuals × Limbic-predominant subtype | 1.22 | 0.72, 2.09 | 0.74 | 0.85 | 0.04, 20.54 | -0.10 |
| Age | 1.03 | 0.99, 1.07 | 1.37 | 1.03 | 0.85, 1.26 | 0.34 |
| Sex | 0.79 | 0.48, 1.31 | -0.91 | 0.80 | 0.09, 6.74 | -0.21 |
| APOE ε4 | 2.28 * * | 1.25, 4.14 | 2.70 | 0.73 | 0.05, 10.00 | -0.23 |
| Observations | 204 | | | 46 | | |
| Number of events | 70 | | | 8 | | |

Hazard ratios (HR) are presented with z-statistics. * $p < 0.05$, * * $p < 0.01$, * ** $p < 0.001$.
Patients who did not progress to dementia within the observation period or did not have follow-up CDR scores were censored.

However, the subtypes in both samples did not significantly differ within respective diagnostic groups with respect to years of education – a common proxy measure of CR (Stern et al., 2020). Alternative variants of CR residuals based on hippocampal and global GM volumes did not show significant differences between the subtypes. Higher CR residuals predicted a slower decline in general cognitive performance and in executive function. Results were suggestive of a potential difference in protective effect of CR between the subtypes. Specifically, the typical subtype seemed to benefit somewhat more from higher CR levels than the limbic-predominant subtype with respect to the longitudinal executive function and global cognitive performance, although the effects were not statistically significant. Further research would be required to confirm these findings and explore potential mechanisms underlying them. Furthermore, we observed differences in longitudinal CR, primarily CR residuals based on hippocampal and global GM volumes, between the hypometabolic subtypes in the main ADNI sample. This result provided support for the link between these sources of heterogeneity in AD. Replication analyses in the ADNI3 sample provided only limited support of results from the main ADNI sample. As in the main ADNI sample, baseline CR residuals and education did not differ between the typical and the limbic-predominant subtypes in ADNI3. Other longitudinal analyses in the ADNI3 sample did not replicate findings from main ADNI sample. However, this is inconclusive likely due to the limited data available in the replication sample.

Current findings demonstrating protective effects of CR are generally in accordance with the previous literature (Nelson et al., 2021). However, specific differences between the hypometabolic subtypes are

**Table 4**
Mixed effects regression models of longitudinal cognitive decline and its relationship with subtypes and CR residuals in the combined CN and prodromal AD group in the main ADNI sample.

| | Memory function composite score | | | Executive function composite score | | | MMSE score | | |
|---|---|---|---|---|---|---|---|---|---|
| | Estimate | CI | t-statistic | Estimate | CI | t-statistic | Estimate | CI | t-statistic |
| Intercept | -0.154 | -0.309, − 0.001 | -1.953 | 0.210 | -0.028, 0.449 | 1.714 | 27.689 * ** | 27.167, 28.214 | 102.761 |
| Age | -0.131 * ** | -0.194, − 0.067 | -4.005 | -0.401 * ** | -0.499, − 0.303 | -7.945 | -0.311 * * | -0.526, − 0.096 | -2.805 |
| Sex | 0.285 * ** | 0.17, 0.4 | 4.824 | 0.038 | -0.142, 0.217 | 0.410 | 0.167 | -0.215, 0.549 | 0.850 |
| APOE ε4 | -0.129 * | -0.201, − 0.103 | -2.123 | -0.226 * | -0.287, − 0.165 | -2.386 | -0.336 | -0.729, 0.058 | -1.663 |
| Follow-up time, years | -0.152 * ** | 0.551, 0.786 | -6.066 | -0.226 * ** | 0.26, 0.623 | -7.246 | -1.232 * ** | -1.58, − 0.884 | -6.905 |
| CR residuals – temporoparietal GM | 0.668 * ** | 0.179, 0.462 | 11.072 | 0.442 * ** | -0.021, 0.416 | 4.733 | 0.711 * ** | 0.302, 1.119 | 3.385 |
| Limbic-predominant subtype | 0.321 * ** | -0.248, − 0.01 | 4.414 | 0.198 | -0.411, − 0.041 | 1.760 | 0.373 | -0.113, 0.857 | 1.496 |
| Follow-up time × Age | -0.004 | -0.033, 0.063 | -0.371 | 0.015 | 0.014, 0.133 | 1.093 | 0.030 | -0.136, 0.197 | 0.353 |
| Follow-up time × CR residuals | 0.015 | -0.034, 0.075 | 0.614 | 0.073 * | 0.039, 0.173 | 2.394 | 0.635 * ** | 0.291, 0.979 | 3.591 |
| Follow-up time × Limbic-predominant subtype | 0.021 | -0.216, 0.056 | 0.746 | 0.106 * * | -0.425, − 0.005 | 3.067 | 0.451 * | 0.058, 0.844 | 2.238 |
| CR residuals× Limbic-predominant subtype | -0.080 | -0.027, 0.018 | -1.146 | -0.215 * | -0.012, 0.042 | -1.987 | -0.132 | -0.601, 0.338 | -0.546 |
| Follow-up time × CR residuals × Limbic-predominant subtype | 0.002 | -0.051, 0.056 | 0.085 | -0.059 | -0.125, 0.007 | -1.750 | -0.376 | -0.763, 0.012 | -1.887 |

Unstandardized estimates are presented with t-statistics. * $p < 0.05$, * * $p < 0.01$, * ** $p < 0.001$. Age variable was centered and rescaled. Random intercepts and slopes are included to account for multiple measurements.

harder to interpret in the context of past research. In our previous study, the limbic-predominant subtype of AD participants included a subcluster showing minimal hypometabolism, as suggested by the hierarchical dendrogram structure (Levin et al., 2021). Additionally, in the current study this subtype tended to have similar or higher temporoparietal GM volume within respective diagnostic groups, compared to the typical subtype. Previous studies considered that a more pronounced neurodegeneration in an AD subtype can correspond to a higher CR because it would allow a person to maintain a specific level of clinical severity despite a subtype of relatively more pronounced neurodegeneration, and the other way around – a subtype with less pronounced neurodegeneration would show lower CR (Ferreira et al., 2020; Persson et al., 2017; Poulakis et al., 2022). Applied to the current study, this interpretation could predict that a subtype with relatively lower neurodegeneration within, for example, the prodromal AD or AD dementia groups would demonstrate lower measures of CR than other participants within the corresponding diagnosis groups. We did not find lower education in the limbic-predominant subtype, but the baseline comparisons suggested somewhat lower average CR residuals (although non-significantly). It should be noted, that selection of specific measures of neurodegeneration and cognitive performance can have an impact on the CR residuals in such baseline comparisons, and the assessment of longitudinal progression is likely more informative.

Our current study primarily focused on comparisons of previously defined hypometabolic subtypes of AD. One potential direction for future research would be to conduct analysis looking at further subdivisions of the subtypes. Identification of more granular AD dementia subtypes that demonstrate reliably higher CR or lower CR than average, in a manner similar to a previous study that examined subtypes of AD resilient to tau pathology (Duong et al., 2022), could contribute to better assessment of individual risk.

We observed different rates of decline of CR residuals between the hypometabolic subtypes in the main ADNI sample. The limbic-predominant subtype showed a slower rate of decline with respect to CR residuals in the main ADNI sample, with a caveat that the effect was not statistically significant for the residuals based on the temporoparietal GM volume. Present findings suggest that the typical subtype as identified in Aβ-positive CN and prodromal AD individuals may be more vulnerable to the depletion of CR. Future research should reconcile this possibility with characteristics of subtypes identified in AD dementia participants and consider longitudinal contributions of differences in protective factors such as CR. An alternative interpretation of the subtype differences with respect to the longitudinal change of CR could be that these differences themselves are caused by the differences in the patterns of neuropathological change. However, evaluation of this possibility would require a different analytical approach than in the current study. In combination with the finding that the limbic-predominant subtype showed a slower longitudinal decrease in temporoparietal GM volume (Supplementary table 10), this also raises a question about a possible contribution of differences in brain maintenance (Stern et al., 2020). Future research in this area could benefit from using a functional measure that would more directly assess mechanisms underlying the CR concept. Another potential future approach to better evaluate and interpret such individual and subtype differences in CR could be to define CR as trajectories of cognitive decline that are better or worse than expected given observed cerebral damage, ideally also examining the continuity of subtypes in Aβ-positive CN, prodromal AD and AD dementia participants.

We addressed the possibility that the CR residual measure could have reflected primarily subtype differences linked to the specific brain areas affected by the neuropathological processes but did not reflect the real CR difference between the subtypes. Thus, we obtained alternative variants of CR residuals using the hippocampal GM and global GM volumes instead of temporoparietal GM. Analyses using these alternative CR residuals yielded similar results (Table 4) suggesting that the selection of the brain area for extracting GM was likely not the driver of subtype differences in CR change. We also repeated the longitudinal regression comparing CR residuals' trajectories between the subtypes in the prodromal AD group only and confirmed that the subtype differences in longitudinal CR residuals change were not driven primarily by the Aβ-positive CN group (Supplementary table 9).

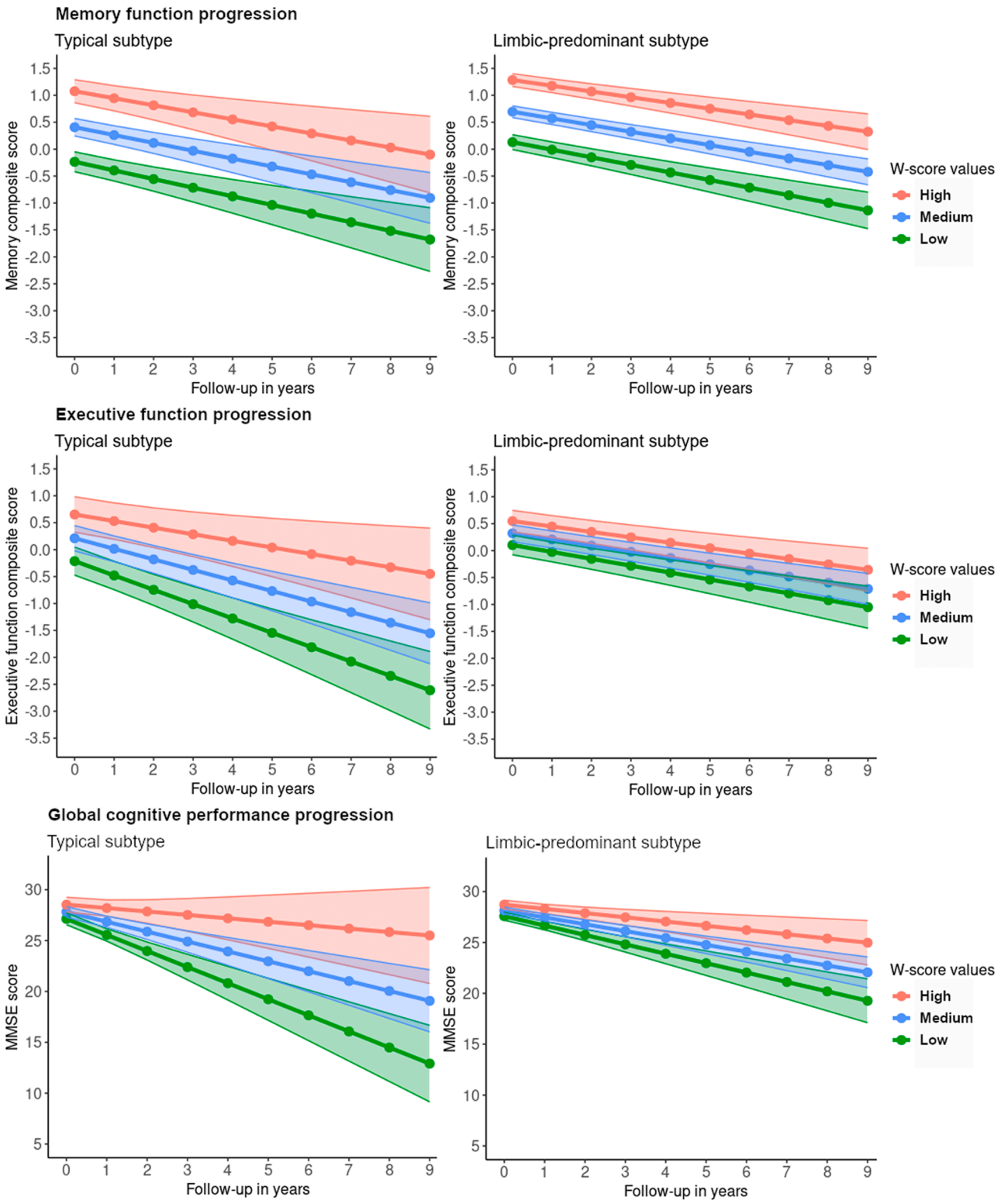


**Fig. 3. Longitudinal cognitive trajectories in Aβ-positive CN and prodromal AD participants depending on CR residuals in the main ADNI sample.** Predicted values of domain-specific cognitive scores were obtained from mixed effects regressions models which included age, sex and APOE ε4, and an interaction of age with the time variable as covariates, as well as random intercepts and slopes to account for multiple measurements. Ribbons around the regression lines represent 95% confidence intervals for the predicted values. Low, medium and high CR residual values were selected as mean values for the lower, medium and higher tertiles of the CR residual distribution respectively.

**Table 5**
Mixed effects regression model of CR residuals in the typical and the limbic-predominant subtypes in Aβ-positive CN and prodromal AD participants in the main ADNI sample.

| | CR residuals – temporoparietal GM | | |
|---|---|---|---|
| | Estimate | CI | t-statistic |
| Intercept | 0.515 * * | 0.167, 0.862 | 2.887 |
| Age | -0.049 | -0.192, 0.094 | -0.672 |
| Sex | -0.079 | -0.341, 0.184 | -0.585 |
| APOE ε4 | -0.543 * ** | -0.808, − 0.279 | -4.029 |
| Scanner change | 0.164 | -0.327, 0.653 | 0.657 |
| Follow-up time, years | -0.127 * | -0.226, − 0.028 | -2.500 |
| Limbic-predominant subtype | 0.269 | -0.056, 0.596 | 1.606 |
| Follow-up time × Age | -0.026 | -0.072, 0.02 | -1.105 |
| Follow-up time × Limbic-predominant subtype | 0.108 | -0.001, 0.217 | 1.942 |

Unstandardized estimates are presented with t-statistics. * $p < 0.05$, * * $p < 0.01$, * ** $p < 0.001$. Age variable was centered and rescaled. Random intercepts and slopes are included to account for multiple measurements. Typical subtype acts as a reference in comparison with the limbic-predominant subtype.

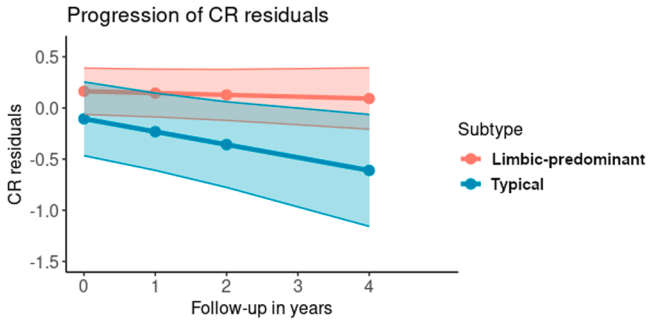


**Fig. 4. Longitudinal trajectories of CR residuals in subtypes in Aβ-positive CN and prodromal AD participants in the main ADNI sample.** Predicted values of residuals were obtained from mixed effects regressions model with age, sex, APOE ε4, a variable indicating a change in the scanner model as covariates and an interaction of age with the time variable, as well as random intercepts and slopes to account for multiple measurements. Ribbons around the regression lines represent 95% confidence intervals for the predicted values.

### *4.1. Potential limitations*

A general limitation of this study, as with other studies applying proxy or residual measures of CR, is that CR is not assessed directly. Rather, it likely captures a number of protective and risk factors that may influence the relationship between observed neuropathology and cognitive performance in addition to the mechanisms underlying individual CR more specifically (Stern et al., 2020). A more direct assessment of brain processes relevant to CR could be possible using functional imaging approaches (Stern et al., 2020).

A relevant limitation of the residual-based approach has been discussed in a recent study by Elman and colleagues (Elman et al., 2022). Specifically, measures of CR operationalized via residual scores tend to correlate with the original dependent variables used in the regression models for obtaining the residual scores – in our case the ADNI-MEM scores. Interpretation of standardized residual scores as measures of CR therefore may be limited and should account for the likely contribution of initial levels of cognitive performance to the variance of the CR measure. In the current study, we primarily focused on group comparisons of the typical and the limbic-predominant subtypes within the prodromal AD group and within the combined group of Aβ-positive CN and prodromal AD. Our finding that the typical and the limbic-predominant subtypes in prodromal AD showed similar levels of CR residuals was unlikely to be confounded by variance in the levels of initial cognitive performance. The subtypes showed similar cognitive performance, and the lack of differences in CR at baseline was supported by a similar finding using the proxy CR measure of education. Thus, the effect of the interaction term including the CR residuals and the subtype on rates of clinical progression and cognitive decline is still informative about potential group level differences in CR. By including these interaction terms, we tested whether the subtypes differed with respect to the protective effect of CR residuals despite similar levels of baseline cognitive performance and CR residuals. Similarly, we used longitudinal regressions in Aβ-positive CN and the prodromal AD participants to assess whether subtypes interacted with CR residuals in analyses predicting cognitive decline. Slower cognitive decline due to higher CR residuals could potentially be attributed to the differences in initial individual cognitive performance. However, the interaction terms including time, CR residuals and subtype suggested that the typical subtype benefited more from higher baseline CR residuals. Finally, we analyzed the longitudinal progression of CR residuals themselves. Results indicated that for the typical subtype CR residuals declined faster than for the limbic-predominant subtype. Our findings suggesting diverging longitudinal trajectories of CR residuals in the subtypes are likely informative beyond differences in the longitudinal cognitive decline and have implications for both subtypes and CR. Specifically, although the subtypes initially demonstrated similar CR, the typical subtype tended to show progressively lower cognitive performance than predicted via a regression model based on a baseline sample of Aβ-positive CN, prodromal AD and AD dementia groups and given the degree of GM atrophy and demographic variables. Thus, the subtype here represents a factor that could potentially account for the variance in cognitive performance that is not sufficiently explained by the longitudinal atrophy. An alternative analytical approach to comparisons of subtypes with respect to longitudinal trajectories of cognitive performance change in response to neurodegeneration could be to evaluate these effects within one longitudinal model. However, due to several complexities of this potential approach such as the limitation of analysis to participants with sufficient longitudinal data, as well as the difficulty of applying an identical CR estimation in a separate sample for replication, here we focused on the more classical approach using CR residuals. To summarize, the recent criticism of the residual-based approach for operationalizing CR may be applicable to findings in participants with higher baseline CR residuals. However, key results from comparisons of the two main subtypes with respect to baseline and longitudinal CR residuals are likely still relevant to understanding the relationship between the subtypes and CR.

Another potential drawback of the current study was the limited available data in the replication sample, including follow-up data, which limited longitudinal statistical testing in this sample. The main challenge in replicating the present analysis was the required combination of FDG-PET, amyloid, longitudinal cognitive and MRI data obtained in various diagnostic groups. Optimization of the current approach to facilitate future research is possible, such as a change in the subtyping approach to using atrophy patterns assessed via MRI to remove the need for FDG-PET.

Finally, the current study used time since baseline as a measure reflecting disease progression in longitudinal regression analyses. Although this measure is often used in similar analyses, this approach could be improved by better accounting for individual disease course, for example via estimation of time since disease onset.

## 5. Conclusion

Here, we evaluated CR in subtypes of AD-related neurodegeneration established previously based on spatial patterns of hypometabolism. Our measure of CR was associated with education and with slower cognitive decline, with a somewhat stronger effect of the levels of CR for the

typical subtype in analyses of cognitive decline. Baseline CR – as assessed by education and by a residual approach – did not support a consistent advantage of a specific subtype, with an exception for the AD group where the limbic-predominant subtype had somewhat lower values of CR residuals. Results suggested that longitudinal CR declined faster for the typical subtype, supporting the hypothesized link between subtype heterogeneity and CR. These findings highlight the importance of considering individual differences in longitudinal CR trajectories. Current results also may inform a better understanding of subtype differences. Further research on CR, as well as on the interplay between CR and subtype heterogeneity, could benefit from more direct assessments of mechanisms underlying CR, as well as from modeling change in CR based on longitudinal cognitive data.

## Ethical approval

Data collection and sharing in ADNI was approved by the Institutional Review Board of each participating institution and all procedures involving human participants were in accordance with the ethical standards of the 1964 Helsinki declaration and its later amendments.

## Funding

MJG is supported by the "Miguel Servet" program [CP19/00031] and a research grant [PI20/00613] of the Instituto de Salud Carlos III-Fondo Europeo de Desarrollo Regional (ISCIII-FEDER).

Authors declare that data contained in the manuscript being submitted have not been previously published, have not been submitted elsewhere and will not be submitted elsewhere while under consideration at Neurobiology of Aging.

All authors have reviewed the contents of the manuscript being submitted, approve of its contents and validate the accuracy of the data.

## CRediT authorship contribution statement

**Teipel Stefan J.:** Conceptualization, Formal analysis, Writing – original draft, Writing – review & editing. **Grothe Michel J.:** Conceptualization, Writing – original draft, Writing – review & editing. **Levin Fedor:** Conceptualization, Formal analysis, Writing – original draft, Writing – review & editing. **Franzmeier Nicolai:** Writing – original draft, Writing – review & editing. **Dyrba Martin:** Writing – original draft, Writing – review & editing.

## Declaration of Competing Interest

SJT participated in scientific advisory boards of Roche Pharma AG, Biogen, Grifols, and MSD, and received lecture fees from Roche and MSD. FL, MJG, MD and NF have no disclosures to report.

## Acknowledgments

MJG is supported by the "Miguel Servet" program [CP19/00031] and a research grant [PI20/00613] of the Instituto de Salud Carlos III-Fondo Europeo de Desarrollo Regional (ISCIII-FEDER).

Data collection and sharing for this project was funded by the Alzheimer's Disease Neuroimaging Initiative (ADNI) (National Institutes of Health Grant U01 AG024904) and DOD ADNI (Department of Defense award number W81XWH-12–2-0012). ADNI is funded by the National Institute on Aging, the National Institute of Biomedical Imaging and Bioengineering, and through generous contributions from the following: AbbVie, Alzheimer's Association; Alzheimer's Drug Discovery Foundation; Araclon Biotech; BioClinica, Inc.; Biogen; Bristol-Myers Squibb Company; CereSpir, Inc.; Cogstate; Eisai Inc.; Elan Pharmaceuticals, Inc.; Eli Lilly and Company; EuroImmun; F. Hoffmann-La Roche Ltd and its affiliated company Genentech, Inc.; Fujirebio; GE Healthcare; IXICO Ltd.; Janssen Alzheimer Immunotherapy Research & Development, LLC.; Johnson & Johnson Pharmaceutical Research & Development LLC.; Lumosity; Lundbeck; Merck & Co., Inc.; Meso Scale Diagnostics, LLC.; NeuroRx Research; Neurotrack Technologies; Novartis Pharmaceuticals Corporation; Pfizer Inc.; Piramal Imaging; Servier; Takeda Pharmaceutical Company; and Transition Therapeutics. The Canadian Institutes of Health Research is providing funds to support ADNI clinical sites in Canada. Private sector contributions are facilitated by the Foundation for the National Institutes of Health (www.fnih.org). The grantee organization is the Northern California Institute for Research and Education, and the study is coordinated by the Alzheimer's Therapeutic Research Institute at the University of Southern California. ADNI data are disseminated by the Laboratory for Neuro Imaging at the University of Southern California.

### *Informed consent*

Written informed consent was obtained from all ADNI participants and/or authorized representatives before any protocol-specific procedures were carried out.

## Appendix A. Supporting information

Supplementary data associated with this article can be found in the online version at doi:10.1016/j.neurobiolaging.2023.12.003.

## References

Bettcher, B.M., Gross, A.L., Gavett, B.E., Widaman, K.F., Fletcher, E., Dowling, N.M., Buckley, R.F., Arenaza-Urquijo, E.M., Zahodne, L.B., Hohman, T.J., Vonk, J.M.J., Rentz, D.M., Mungas, D., 2019. Dynamic change of cognitive reserve: associations with changes in brain, cognition, and diagnosis. Neurobiol. Aging 83, 95–104. https://doi.org/10.1016/j.neurobiolaging.2019.08.016.

Crane, P.K., Carle, A., Gibbons, L.E., Insel, P., Mackin, R.S., Gross, A., Jones, R.N., Mukherjee, S., Curtis, S.M., Harvey, D., Weiner, M., Mungas, D., 2012. Development and assessment of a composite score for memory in the Alzheimer's Disease Neuroimaging Initiative (ADNI). Brain Imaging Behav. 6 (4), 502–516. https://doi.org/10.1007/s11682-012-9186-z.

Duong, M.T., Das, S.R., Lyu, X., Xie, L., Richardson, H., Xie, S.X., Yushkevich, P.A., Weiner, M., Aisen, P., Petersen, R., Jack, C.R., Jagust, W., Trojanowki, J.Q., Toga, A. W., Beckett, L., Green, R.C., Saykin, A.J., Morris, J.C., Shaw, L.M., Liu, E., Montine, T., Thomas, R.G., Donohue, M., Walter, S., Gessert, D., Sather, T., Jimenez-Maggiora, G., Harvey, D., Bernstein, M., Fox, N., Thompson, P., Schuff, N., DeCarli, C., Borowski, B., Gunter, J., Senjem, M., Vemuri, P., Jones, D., Kantarci, K., Ward, C., Koeppe, R.A., Foster, N., Reiman, E.M., Chen, K., Mathis, C., Landau, S., Cairns, N.J., Householder, E., Taylor-Reinwald, L., Lee, V.M.Y., Korecka, M., Figurski, M., Crawford, K., Neu, S., Foroud, T.M., Shen, L., Faber, K., Kim, S., Nho, K., Khachaturian, Z., Frank, R., Snyder, P.J., Molchan, S., Kaye, J., Quinn, J., Lind, B., Carter, R., Dolen, S., Schneider, L.S., Pawluczyk, S., Beccera, M., Teodoro, L., Spann, B.M., Brewer, J., Vanderswag, H., Fleisher, A., Heidebrink, J.L., Lord, J.L., Mason, S.S., Albers, C.S., Knopman, D., Johnson, K., Doody, R.S., Villanueva-Meyer, J., Chowdhury, M., Rountree, S., Dang, M., Stern, Y., Honig, L.S., Bell, K.L., Ances, B., Carroll, M., Leon, S., Mintun, M.A., Schneider, S., Oliver, A., Griffith, R., Clark, D., Geldmacher, D., Brockington, J., Roberson, E., Grossman, H., Mitsis, E., deToledo-Morrell, L., Shah, R.C., Duara, R., Varon, D., Greig, M.T., Roberts, P., Albert, M., Onyike, C., D'Agostino, D., Kielb, S., Galvin, J.E., Pogorelec, D.M., Cerbone, B., Michel, C.A., Rusinek, H., de Leon, M.J., Glodzik, L., De Santi, S., Doraiswamy, P.M., Petrella, J.R., Wong, T.Z., Clark, C.M., Arnold, S.E., Karlawish, J.H., Wolk, D.A., Smith, C.D., Jicha, G., Hardy, P., Sinha, P., Oates, E., Conrad, G., Lopez, O.L., Oakley, M., Simpson, D.M., Porsteinsson, A.P., Goldstein, B. S., Martin, K., Makino, K.M., Ismail, M.S., Brand, C., Mulnard, R.A., Thai, G., McAdams-Ortiz, C., Womack, K., Mathews, D., Quiceno, M., Diaz-Arrastia, R., King, R., Weiner, M., Cook, K.M., Devous, M., Levey, A.I., Lah, J.J., Cellar, J.S., Burns, J.M., Anderson, H.S., Swerdlow, R.H., Apostolova, L., Tingus, K., Woo, E., Silverman, D.H.S., Lu, P.H., Bartzokis, G., Graff-Radford, N.R., Parfitt, F., Kendall, T., Johnson, H., Farlow, M.R., Hake, A.M., Matthews, B.R., Herring, S., Hunt, C., van Dyck, C.H., Carson, R.E., MacAvoy, M.G., Chertkow, H., Bergman, H., Hosein, C., Black, S., Stefanovic, B., Caldwell, C., Hsiung, G.-Y.R., Feldman, H., Mudge, B., Assaly, M., Kertesz, A., Rogers, J., Bernick, C., Munic, D., Kerwin, D., Mesulam, M. M., Lipowski, K., Wu, C.-K., Johnson, N., Sadowsky, C., Martinez, W., Villena, T., Turner, R.S., Johnson, K., Reynolds, B., Sperling, R.A., Johnson, K.A., Marshall, G., Frey, M., Yesavage, J., Taylor, J.L., Lane, B., Rosen, A., Tinklenberg, J., Sabbagh, M. N., Belden, C.M., Jacobson, S.A., Sirrel, S.A., Kowall, N., Killiany, R., Budson, A.E., Norbash, A., Johnson, P.L., Obisesan, T.O., Wolday, S., Allard, J., Lerner, A., Ogrocki, P., Hudson, L., Fletcher, E., Carmichael, O., Olichney, J., Kittur, S., Borrie, M., Lee, T.Y., Bartha, R., Johnson, S., Asthana, S., Carlsson, C.M., Potkin, S. G., Preda, A., Nguyen, D., Tariot, P., Reeder, S., Bates, V., Capote, H., Rainka, M., Scharre, D.W., Kataki, M., Adeli, A., Zimmerman, E.A., Celmins, D., Brown, A.D., Pearlson, G.D., Blank, K., Anderson, K., Santulli, R.B., Kitzmiller, T.J., Schwartz, E.S.,

Sink, K.M., Williamson, J.D., Garg, P., Watkins, F., Ott, B.R., Querfurth, H., Tremont, G., Salloway, S., Malloy, P., Correia, S., Rosen, H.J., Miller, B.L., Mintzer, J., Spicer, K., Bachman, D., Finger, E., Pasternak, S., Rachinsky, I., Drost, D., Pomara, N., Hernando, R., Sarrael, A., Schultz, S.K., Boles Ponto, L.L., Shim, H., Smith, K.E., Relkin, N., Chiang, G., Ravdin, L., Smith, A., Fargher, K., Raj, B.A., Wolk, D.A., Nasrallah, I.M., 2022. Dissociation of tau pathology and neuronal hypometabolism within the ATN framework of Alzheimer's disease. Nat. Commun. 13 (1) https://doi.org/10.1038/s41467-022-28941-1.

Dyrba, M., Hanzig, M., Altenstein, S., Bader, S., Ballarini, T., Brosseron, F., Buerger, K., Cantré, D., Dechent, P., Dobisch, L., Düzel, E., Ewers, M., Fliessbach, K., Glanz, W., Haynes, J.-D., Heneka, M.T., Janowitz, D., Keles, D.B., Kilimann, I., Laske, C., Maier, F., Metzger, C.D., Munk, M.H., Perneczky, R., Peters, O., Preis, L., Priller, J., Rauchmann, B., Roy, N., Scheffler, K., Schneider, A., Schott, B.H., Spottke, A., Spruth, E.J., Weber, M.-A., Ertl-Wagner, B., Wagner, M., Wiltfang, J., Jessen, F., Teipel, S.J., 2021. Improving 3D convolutional neural network comprehensibility via interactive visualization of relevance maps: evaluation in Alzheimer's disease. Alzheimer'S. Res. Ther. 13 (1) https://doi.org/10.1186/s13195-021-00924-2.

Elman, J.A., Vogel, J.W., Bocancea, D.I., Ossenkoppele, R., van Loenhoud, A.C., Tu, X.M., Kremen, W.S., 2022. Issues and recommendations for the residual approach to quantifying cognitive resilience and reserve. Alzheimer'S. Res. Ther. 14 (1) https://doi.org/10.1186/s13195-022-01049-w.

Ewers, M., Luan, Y., Frontzkowski, L., Neitzel, J., Rubinski, A., Dichgans, M., Hassenstab, J., Gordon, B.A., Chhatwal, J.P., Levin, J., Schofield, P., Benzinger, T.L. S., Morris, J.C., Goate, A., Karch, C.M., Fagan, A.M., McDade, E., Allegri, R., Berman, S., Chui, H., Cruchaga, C., Farlow, M., Graff-Radford, N., Jucker, M., Lee, J.-H., Martins, R.N., Mori, H., Perrin, R., Xiong, C., Rossor, M., Fox, N.C., O'Connor, A., Salloway, S., Danek, A., Buerger, K., Bateman, R.J., Habeck, C., Stern, Y., Franzmeier, N., 2021. Segregation of functional networks is associated with cognitive resilience in Alzheimer's disease. Brain 144 (7), 2176–2185. https://doi.org/10.1093/brain/awab112.

Ferreira, D., Nordberg, A., Westman, E., 2020. Biological subtypes of Alzheimer disease. Neurology 94 (10), 436–448. https://doi.org/10.1212/wnl.0000000000009058.

Franzmeier, N., Duering, M., Weiner, M., Dichgans, M., Ewers, M., 2017. Left frontal cortex connectivity underlies cognitive reserve in prodromal Alzheimer disease. Neurology 88 (11), 1054–1061. https://doi.org/10.1212/wnl.0000000000003711.

Franzmeier, N., Düzel, E., Jessen, F., Buerger, K., Levin, J., Duering, M., Dichgans, M., Haass, C., Suárez-Calvet, M., Fagan, A.M., Paumier, K., Benzinger, T., Masters, C.L., Morris, J.C., Perneczky, R., Janowitz, D., Catak, C., Wolfsgruber, S., Wagner, M., Teipel, S., Kilimann, I., Ramirez, A., Rossor, M., Jucker, M., Chhatwal, J., Spottke, A., Boecker, H., Brosseron, F., Falkai, P., Fliessbach, K., Heneka, M.T., Laske, C., Nestor, P., Peters, O., Fuentes, M., Menne, F., Priller, J., Spruth, E.J., Franke, C., Schneider, A., Kofler, B., Westerteicher, C., Speck, O., Wiltfang, J., Bartels, C., Araque Caballero, M.Á., Metzger, C., Bittner, D., Weiner, M., Lee, J.-H., Salloway, S., Danek, A., Goate, A., Schofield, P.R., Bateman, R.J., Ewers, M., 2018. Left frontal hub connectivity delays cognitive impairment in autosomal-dominant and sporadic Alzheimer's disease. Brain 141 (4), 1186–1200. https://doi.org/10.1093/brain/awy008.

Franzmeier, N., Dewenter, A., Frontzkowski, L., Dichgans, M., Rubinski, A., Neitzel, J., Smith, R., Strandberg, O., Ossenkoppele, R., Buerger, K., Duering, M., Hansson, O., Ewers, M., 2020. Patient-centered connectivity-based prediction of tau pathology spread in Alzheimer's disease. Sci. Adv. 6 (48) https://doi.org/10.1126/sciadv.abd1327.

Gaser, C., Dahnke, R., Thompson, P.M., Kurth, F., Luders, E., 2023. CAT - A Computational Anatomy Toolbox for the Analysis of Structural MRI Data. BioRxiv. https://doi.org/10.1101/2022.06.11.495736 [PREPRINT].

Gibbons, L.E., Carle, A.C., Mackin, R.S., Harvey, D., Mukherjee, S., Insel, P., Curtis, S.M., Mungas, D., Crane, P.K., 2012. A composite score for executive functioning, validated in Alzheimer's Disease Neuroimaging Initiative (ADNI) participants with baseline mild cognitive impairment. Brain Imaging Behav. 6 (4), 517–527. https://doi.org/10.1007/s11682-012-9176-1.

Grothe, M.J., Moscoso, A., Ashton, N.J., Karikari, T.K., Lantero-Rodriguez, J., Snellman, A., Zetterberg, H., Blennow, K., Schöll, M., 2021. Associations of fully automated CSF and novel plasma biomarkers with alzheimer disease neuropathology at autopsy. Neurology 97 (12), e1229–e1242. https://doi.org/10.1212/wnl.0000000000012513.

Habes, M., Grothe, M.J., Tunc, B., McMillan, C., Wolk, D.A., Davatzikos, C., 2020. Disentangling heterogeneity in Alzheimer's disease and related dementias using data-driven methods. Biol. Psychiatry 88 (1), 70–82. https://doi.org/10.1016/j.biopsych.2020.01.016.

Hansson, O., Seibyl, J., Stomrud, E., Zetterberg, H., Trojanowski, J.Q., Bittner, T., Lifke, V., Corradini, V., Eichenlaub, U., Batrla, R., Buck, K., Zink, K., Rabe, C., Blennow, K., Shaw, L.M., 2018. CSF biomarkers of Alzheimer's disease concord with amyloid-β PET and predict clinical progression: a study of fully automated immunoassays in BioFINDER and ADNI cohorts. Alzheimer'S. Dement. 14 (11), 1470–1481. https://doi.org/10.1016/j.jalz.2018.01.010.

Jack, C.R., Petersen, R.C., Xu, Y.C., Waring, S.C., O'Brien, P.C., Tangalos, E.G., Smith, G. E., Ivnik, R.J., Kokmen, E., 1997. Medial temporal atrophy on MRI in normal aging and very mild Alzheimer's disease. Neurology 49 (3), 786–794. https://doi.org/10.1212/wnl.49.3.786.

Kljajevic, V., Grothe, M.J., Ewers, M., Teipel, S., 2014. Distinct pattern of hypometabolism and atrophy in preclinical and predementia Alzheimer's disease. Neurobiol. Aging 35 (9), 1973–1981. https://doi.org/10.1016/j.neurobiolaging.2014.04.006.

Lam, B., Masellis, M., Freedman, M., Stuss, D.T., Black, S.E., 2013. Clinical, imaging, and pathological heterogeneity of the Alzheimer's disease syndrome. Alzheimer'S. Res. Ther. 5 (1) https://doi.org/10.1186/alzrt155.

Landau, S.M., Thomas, B.A., Thurfjell, L., Schmidt, M., Margolin, R., Mintun, M., Pontecorvo, M., Baker, S.L., Jagust, W.J., 2014. Amyloid PET imaging in Alzheimer's disease: a comparison of three radiotracers. Eur. J. Nucl. Med. Mol. Imaging 41 (7), 1398–1407. https://doi.org/10.1007/s00259-014-2753-3.

Lange, C., Suppa, P., Frings, L., Brenner, W., Spies, L., Buchert, R., 2016. Optimization of statistical single subject analysis of brain FDG PET for the prognosis of mild cognitive impairment-to-Alzheimer's disease conversion. J. Alzheimer'S. Dis. 49 (4), 945–959. https://doi.org/10.3233/jad-150814.

Levin, F., Ferreira, D., Lange, C., Dyrba, M., Westman, E., Buchert, R., Teipel, S.J., Grothe, M.J., 2021. Data-driven FDG-PET subtypes of Alzheimer's disease-related neurodegeneration. Alzheimer'S. Res. Ther. 13 (1) https://doi.org/10.1186/s13195-021-00785-9.

Nelson, M.E., Jester, D.J., Petkus, A.J., Andel, R., 2021. Cognitive reserve, Alzheimer's neuropathology, and risk of dementia: a systematic review and meta-analysis. Neuropsychol. Rev. 31 (2), 233–250. https://doi.org/10.1007/s11065-021-09478-4.

Ossenkoppele, R., Cohn-Sheehy, B.I., La Joie, R., Vogel, J.W., Möller, C., Lehmann, M., van Berckel, B.N.M., Seeley, W.W., Pijnenburg, Y.A., Gorno-Tempini, M.L., Kramer, J.H., Barkhof, F., Rosen, H.J., van der Flier, W.M., Jagust, W.J., Miller, B.L., Scheltens, P., Rabinovici, G.D., 2015. Atrophy patterns in early clinical stages across distinct phenotypes of Alzheimer's disease. Hum. Brain Mapp. 36 (11), 4421–4437. https://doi.org/10.1002/hbm.22927.

Persson, K., Eldholm, R.S., Barca, M.L., Cavallin, L., Ferreira, D., Knapskog, A.-B., Selbæk, G., Brækhus, A., Saltvedt, I., Westman, E., Engedal, K., 2017. MRI-assessed atrophy subtypes in Alzheimer's disease and the cognitive reserve hypothesis. Plos One 12 (10). https://doi.org/10.1371/journal.pone.0186595.

Poulakis, K., Pereira, J.B., Muehlboeck, J.S., Wahlund, L.-O., Smedby, Ö., Volpe, G., Masters, C.L., Ames, D., Niimi, Y., Iwatsubo, T., Ferreira, D., Westman, E., 2022. Multi-cohort and longitudinal Bayesian clustering study of stage and subtype in Alzheimer's disease. Nat. Commun. 13 (1) https://doi.org/10.1038/s41467-022-32202-6.

Reed, B.R., Mungas, D., Farias, S.T., Harvey, D., Beckett, L., Widaman, K., Hinton, L., DeCarli, C., 2010. Measuring cognitive reserve based on the decomposition of episodic memory variance. Brain 133 (8), 2196–2209. https://doi.org/10.1093/brain/awq154.

Rolls, E.T., Huang, C.-C., Lin, C.-P., Feng, J., Joliot, M., 2020. Automated anatomical labelling atlas 3. NeuroImage 206. https://doi.org/10.1016/j.neuroimage.2019.116189.

Royse, S.K., Minhas, D.S., Lopresti, B.J., Murphy, A., Ward, T., Koeppe, R.A., Bullich, S., DeSanti, S., Jagust, W.J., Landau, S.M., 2021. Validation of amyloid PET positivity thresholds in centiloids: a multisite PET study approach. Alzheimer'S. Res. Ther. 13 (1) https://doi.org/10.1186/s13195-021-00836-1.

Saykin, A.J., Shen, L., Foroud, T.M., Potkin, S.G., Swaminathan, S., Kim, S., Risacher, S. L., Nho, K., Huentelman, M.J., Craig, D.W., Thompson, P.M., Stein, J.L., Moore, J.H., Farrer, L.A., Green, R.C., Bertram, L., Jack, C.R., Weiner, M.W., 2010. Alzheimer's Disease Neuroimaging Initiative biomarkers as quantitative phenotypes: genetics core aims, progress, and plans. Alzheimer'S. Dement. 6 (3), 265–273. https://doi.org/10.1016/j.jalz.2010.03.013.

Stern, Y., 2002. What is cognitive reserve? Theory and research application of the reserve concept. J. Int. Neuropsychol. Soc. 8 (3), 448–460. https://doi.org/10.1017/s1355617702813248.

Stern, Y., 2012. Cognitive reserve in ageing and Alzheimer's disease. Lancet Neurol. 11 (11), 1006–1012. https://doi.org/10.1016/s1474-4422(12)70191-6.

Stern, Y., Arenaza-Urquijo, E.M., Bartrés-Faz, D., Belleville, S., Cantilon, M., Chetelat, G., Ewers, M., Franzmeier, N., Kempermann, G., Kremen, W.S., Okonkwo, O., Scarmeas, N., Soldan, A., Udeh-Momoh, C., Valenzuela, M., Vemuri, P., Vuoksimaa, E., 2020. Whitepaper: Defining and investigating cognitive reserve, brain reserve, and brain maintenance. Alzheimer'S. Dement. 16 (9), 1305–1311. https://doi.org/10.1016/j.jalz.2018.07.219.

Teipel, S., Grothe, M.J., 2015. Does posterior cingulate hypometabolism result from disconnection or local pathology across preclinical and clinical stages of Alzheimer's disease? Eur. J. Nucl. Med. Mol. Imaging 43 (3), 526–536. https://doi.org/10.1007/s00259-015-3222-3.

Teipel, S.J., Dyrba, M., Chiesa, P.A., Sakr, F., Jelistratova, I., Lista, S., Vergallo, A., Lemercier, P., Cavedo, E., Habert, M.O., Dubois, B., Hampel, H., Grothe, M.J., 2020. In vivo staging of regional amyloid deposition predicts functional conversion in the preclinical and prodromal phases of Alzheimer's disease. Neurobiol. Aging 93, 98–108. https://doi.org/10.1016/j.neurobiolaging.2020.03.011.

Tzourio-Mazoyer, N., Landeau, B., Papathanassiou, D., Crivello, F., Etard, O., Delcroix, N., Mazoyer, B., Joliot, M., 2002. Automated anatomical labeling of activations in spm using a macroscopic anatomical parcellation of the MNI MRI single-subject brain. NeuroImage 15 (1), 273–289. https://doi.org/10.1006/nimg.2001.0978.

van Loenhoud, A.C., Wink, A.M., Groot, C., Verfaillie, S.C.J., Twisk, J., Barkhof, F., van Berckel, B., Scheltens, P., van der Flier, W.M., Ossenkoppele, R., 2017. A neuroimaging approach to capture cognitive reserve: application to Alzheimer's disease. Hum. Brain Mapp. 38 (9), 4703–4715. https://doi.org/10.1002/hbm.23695.

van Loenhoud, A.C., van der Flier, W.M., Wink, A.M., Dicks, E., Groot, C., Twisk, J., Barkhof, F., Scheltens, P., Ossenkoppele, R., 2019. Cognitive reserve and clinical

progression in Alzheimer disease. Neurology 93 (4), e334–e346. https://doi.org/10.1212/wnl.0000000000007821.

Vogel, J.W., Young, A.L., Oxtoby, N.P., Smith, R., Ossenkoppele, R., Strandberg, O.T., La Joie, R., Aksman, L.M., Grothe, M.J., Iturria-Medina, Y., Pontecorvo, M.J., Devous, M.D., Rabinovici, G.D., Alexander, D.C., Lyoo, C.H., Evans, A.C., Hansson, O., 2021. Four distinct trajectories of tau deposition identified in Alzheimer's disease. Nat. Med. 27 (5), 871–881. https://doi.org/10.1038/s41591-021-01309-6.

Zahodne, L.B., Manly, J.J., Brickman, A.M., Narkhede, A., Griffith, E.Y., Guzman, V.A., Schupf, N., Stern, Y., 2015. Is residual memory variance a valid method for quantifying cognitive reserve? A longitudinal application. Neuropsychologia 77, 260–266. https://doi.org/10.1016/j.neuropsychologia.2015.09.009.